Photosynthesis and net primary productivity in three Antarctic diatoms: possible significance for their distribution in the Antarctic marine ecosystem

K. Petrou*, P. J. Ralph

Plant Functional Biology and Climate Change Cluster and School of Environment, University of Technology, Sydney, PO Box 123, Broadway, New South Wales, 2007, Australia.

*Corresponding author:

Katherina Petrou email: klpetrou@uts.edu.au

Running head: Primary productivity in Antarctic diatoms

Abstract

Photosynthesis and net primary productivity were measured in three Antarctic diatoms, *Fragilariopsis cylindrus*, *Pseudo-nitzschia subcurvata* and *Chaetoceros* sp., exposed to rapid changes in temperature and salinity representing a range of conditions found during a seasonal cycle. Measured differences in fluorescence-derived photosynthetic activity and oxygen evolution suggested some alternative electron cycling activity present under high irradiances. *Fragilariopsis cylindrus* displayed the highest rates of relative electron transport and net primary productivity under all salinity and temperature combinations and showed adaptive traits towards the sea ice-like environment. *Pseudo-nitzschia subcurvata* displayed a preference for low saline conditions where production rates were greatest. However, there was evidence of photosynthetic sensitivity to the lowest temperatures and highest salinities, suggesting a lack of adaptation for dealing with sea ice-like conditions. *Chaetoceros* sp. showed high plasticity, acclimating well to all conditions, but performing best under pelagic conditions. The study shows species-specific sensitivities to environmental change highlighting photosynthetic capacity as a potentially important mechanism in ecological niche adaptation. When these data were modelled over different seasons, integrated daily net primary production was greatest under summer pelagic conditions. The findings from this study support the general observations of light control and seasonal development of net primary productivity and species succession in the Antarctic marine ecosystem.

Introduction

Numerous studies have linked phytoplankton physiology with ecological adaptation (Sakshaug et al 1987; Strzepek and Harrison 2004; Bailey et al 2008). Such studies have found that the photosynthetic architecture and physiology of species can differ greatly and adaptive traits can be linked to the species' ability to inhabit and often dominate a particular ecological niche, including niche occupancy as a function of light (Sakshaug et al 1987; Lavaud et al 2007), iron availability (Strzepek and Harrison 2004; Bailey et al 2008, Mackey et al 2008) and photoprotective capacity (Dimier et al 2009). In particular, the ecological success of diatoms has been linked with a high photosynthetic flexibility, allowing this class of microalgae to outcompete other phytoplankton groups, especially in environments where light is variable (Kashino et al 2002; Wagner et al 2006). Indeed, even within the diatom group, there have been measurable differences in short-term acclimation strategies and photoprotective capacity between individual species from different environments (Dimier et al 2007; Lavaud et al 2007). The large diversity in diatom physiological plasticity and ecological niche selectivity, suggests that Antarctic diatoms in general should be adapted to such variable and extreme conditions and therefore should display high photoprotective capabilities. However, little is known whether differences in photoprotective capacity among Antarctic diatom species can be linked with specific niche environments.

Antarctic marine phytoplankton are exposed to large changes in ecosystem conditions during an annual cycle (Fig. 1). In winter, phytoplankton are rapidly incorporated into the sea ice matrix where they are confined to tiny brine channels (salinities up to 145) at freezing temperatures (Gleitz and Thomas 1992). Initially incoming solar irradiance is very high in the developing sea ice, as a result of being constrained close to the surface, but as the ice thickens, irradiance declines, often to levels of less than 1% surface irradiance (Palmisano et

67 al 1987). In the austral spring, the ice begins to melt, and the microalgae are washed out of
68 the brine channels into a surface lens of hyposaline water. The meltwater environment,
69 characterised by low salinities (typically below 33), a stable water column and shallow mixed
70 layer, forms an ideal environment for the development of phytoplankton blooms (Dierssen et
71 al 2002). In summer, the Southern Ocean mixes phytoplankton from the surface waters to the
72 deep, delivering a moderate and variable light environment, warmer temperatures and
73 moderate salinity (Fig. 1). All of these shifts in light, temperature and salinity, can have a
74 profound effect on phytoplankton growth rates (Aletsee and Jahnke 1992) and carbon
75 assimilation (Thomas and Gleitz 1993). High carbon turnover has been associated with fast
76 growing Antarctic diatoms (Thomas and Gleitz 1993) and growth rates under low
77 temperature/high salinity conditions have been shown to differ between Antarctic diatom
78 species (Aletsee and Jahnke 1992). Therefore it follows that photosynthesis under different
79 environmental conditions will be species-specific, this in turn, would result in differences in
80 species' contributions to the community net primary productivity.

81 Traditionally, ^{14}C-uptake and oxygen evolution were used to estimate primary
82 production and photosynthesis (Juneau and Harrison 2005). However, in recent decades
83 chlorophyll *a* fluorescence has been a popular technique employed to investigate the
84 photophysiology of plants (Krause and Weiss 1991). Several studies have found a good
85 correlation between fluorescence-derived relative electron transport rates with primary
86 productivity measured as oxygen evolution or carbon fixation under low light conditions
87 (Geel et al 1997; Prasil et al 1996; Masojidek et al 2001). In all cases, linearity disappears
88 beyond light saturation levels, resulting in fluorescence data vastly over-estimating primary
89 production (Gilbert et al 2000). In diatoms, there have been several alternative electron
90 pathways, not leading to carbon fixation, suggested as possible reasons behind this

discrepancy, including cyclic electron transport around PSII (Prasil et al 1996; Lavaud et al 2002), cyclic electron transport around PSI (Bendall and Manesse 1995) and the water-water cycle (Geel et al 1997).

The physical and biological processes associated with the seasonal formation and decay of sea ice is what shapes Antarctic phytoplankton communities, determining colonisation, growth, succession, grazing and ultimately, productivity. This study investigates short-term acclimation in photosynthesis and net primary production in three Antarctic diatoms exposed to rapid shifts in temperature and salinity simulating transient environmental conditions of seasonal relevance (sea ice, meltwater and pelagic environments). It measures net primary productivity (measured as oxygen evolution) and electron transport efficiency (measured using chlorophyll *a* fluorescence), and investigates species-specific physiological sensitivities to rapid changes in temperature and salinity. Furthermore, it discusses how this may influence species-specific contributions to overall primary productivity within the Antarctic marine ecosystem. It is hypothesised that species known to dominate a particular niche environment will show physiological adaptation and rapid acclimation to those conditions. Net primary productivity will vary between species under different environmental conditions and species displaying a low photosynthetic plasticity will express photosynthetic sensitivity to conditions outside their preferred ecological niche.

Materials and Methods

Cultures and sampling

The Antarctic diatom *Fragilariopsis cylindrus* (Grunow) was collected from ice cores (66°S, 147°E) taken in November 2001, *Chaetoceros* sp. was isolated from East Antarctic

coastal waters, and *Pseudo-nitszchia subcurvata* (Hasle) Fryxell PS71/60-1 Plate II B1 was collected from the subpolar South Atlantic ocean (58°S). Diatoms were cultured in natural seawater (salinity 34) enriched with F/2 nutrients in specialised glass bottles (approx. 1 L) under continuous air bubbling and maintained at +4°C (Guillard and Ryther 1962). Light was supplied at 50 µmol photons m^{-2} s^{-1} (Grolux, GMT lighting, Northmead, Australia) on a 16:8 light:dark cycle. For simplicity, one, moderate light level was used in all treatments throughout the experiment to avoid confounding any responses to the salinity and temperature treatments. Once reaching exponential growth phase, measured using in vivo fluorescence (Trilogy, Turner Designs Inc., Sunnyvale CA, United States of America (U.S.A)), cultures were maintained semi-continuously diluting (up to 90% with fresh media) periodically to keep cells in exponential phase for the duration of the experiment. For experimental treatments, cells from independent culture flasks (representing replicates) were gently filter-concentrated above 2 µm polycarbonate membrane filters (Millipore, MA, USA) and resuspended into 250 mL culture flasks. At each temperature treatment (-1.5, +2 and +5°C (± 0.3°C)) cells were transferred into four salinities, 31, 34, 55 and 70 (± 0.5) and were given 72 h in their new conditions before measurements were made. A 3-day acclimation period was chosen in order to investigate short-term acclimation strategies of three diatom species during a rapid freezing or thawing event. Salinities were adjusted either by the addition of MilliQ water or sodium chloride (NaCl) salt (Sigma, USA) and were confirmed by refractometer.

Chlorophyll a *fluorescence*

Fluorescence-based estimates of photosynthesis were measured using Pulse Amplitude Modulated fluorometer (Water-PAM; Walz GmbH, Effeltrich, Germany). A 3 ml

aliquot of each treatment was transferred into a quartz cuvette and maintained under continuous stirring to prevent settling. After 5 min dark-adaptation, minimum (F_O) and maximum (F_M) fluorescence were obtained. This was followed by the sequential application of nine actinic light levels (28, 42, 65, 100, 150, 320, 680, 1220 and 2260 μmol photons m^{-2} s^{-1}) applied for 5 min each, with saturating pulses of light (pulse duration = 0.6 s; pulse intensity > 3000 μmol photons m^{-2} s^{-1}) applied every minute. Relative electron transport rate (rETR) was calculated as the product of effective quantum yield (φ_{PSII}) and irradiance (μmol photons m^{-2} s^{-1}) and normalised to chlorophyll *a* concentration (mg L^{-1}).

Oxygen evolution

Oxygen uptake and evolution were measured using a 24-well plate reader optode system (Pre Sens, Precision Sensing GmbH, Regensburg, Germany). Aliquots (3 mL) of filter-concentrated cultures (3 fold) were transferred into 36 wells of two 24-well plates and left in the dark for 30 min while oxygen consumption was monitored. Cells were then incubated at nine light levels (20, 40, 65, 100, 160, 300, 600, 1100, 2250 μmol photons m^{-2} s^{-1}) for 1 h (for each irradiance) and oxygen evolution rate determined. Light levels were attained by covering the well plate lids with neutral density filters and light provided by a non-heat radiating light source (Zeiss KL2500, Zeiss, Germany). Oxygen flux measurements (μmol O_2 L^{-1} h^{-1}) were used to calculate net primary production rates at each light level and data were normalised to chl *a* (mg L^{-1}) concentration. All fluorescence and oxygen measurements were conducted at each corresponding treatment temperature.

Chlorophyll a *concentration*

Chlorophyll *a* concentrations for fluorescence and oxygen measurements were determined by filtering (10 mL) samples onto 25 mm GF/F filters (Whatman, USA),

immediately frozen in liquid nitrogen and stored in the dark at -80˚C for later analysis. Pigments were extracted in 90% acetone and left in the dark at 4°C for 24 h. Pigment concentrations were measured on a spectrophotometer (Cary 50, Varian, CA, USA) at wavelengths 750, 664 and 630 nm and calculated according to Ritchie (2006).

Data analysis

Relative ETR and oxygen evolution data were plotted according to the different temperature and salinity conditions experienced in the Antarctic; although not perfectly representative of the natural world, salinity and temperature treatments were combined to correspond to different Antarctic ecological niche environments: sea ice (-1.5°C at 70), meltwater (+2°C at 31) and pelagic (+5°C at 34; Fig. 1). Oxygen evolution and fluorescence data were fitted according to a double exponential function as in Ralph and Gademann (2005). All photosynthetic parameters derived from the oxygen and fluorescence data including: maximum rate of oxygen evolution (O_{2max}), light utilisation efficiency (α), minimum saturating irradiances (E_K), optimal photosynthetic irradiance (E_M), photoinhibitory irradiance (E_B) and maximum electron transport rate (ETR_{max}), were obtained from these curves following Ralph and Gademann (2005). Photosynthetic and NPP parameters were tested for statistical significance between species (*F. cylindrus*, *P. subcurvata* and *Chaetoceros* sp.) and environments (sea ice, meltwater and pelagic) using a two-factor ANOVA with Tukey's *post hoc* comparisons ($\alpha = 0.05$). All data were tested for homoscedasticity prior to analysis. The data for the photosynthetic parameters α_{O2} and E_{kO2} were log transformed to meet assumptions of ANOVA. Least squares linear regression was used to determine the relationship between rETR and oxygen evolution rates for all data values below and those above minimum saturating irradiance (E_K). To further investigate

187 species-specific sensitivity to changes in temperature and salinity, photosynthetic parameters
188 α_{O2}, $E_{K\,O2}$ and O_{2max} from oxygen evolution data were plotted as a contour graph using the
189 entire matrix of four salinities (31, 34, 55, and 70) and three temperatures (-1.5, +2, and
190 +5°C) that were tested.
191
192 *Net primary production estimates*

193 To place these results in a broader and more ecologically relevant context, the
194 parameters derived from the light response curves were used to estimate daily integrated net
195 primary production [μmol O_2 (mg chl *a*)$^{-1}$ d^{-1}] for each species under each environmental
196 condition. Daily surface irradiance was computed as a bell shaped curve with a noon
197 maximum irradiance and a photoperiod typical of each environment derived from literature
198 values (Table 1; Fig. 2). Data on the monthly photoperiod for each environmental condition
199 was taken from www.esrl.noaa.gov/gmd/grad/solcalc which are based on the astronomical
200 algorithms of Jean Meeus (Earth System Research Laboratory, National Oceanic &
201 Atmospheric Administration) using latitude (065°S) and longitude (145°E) of the east
202 Antarctic seasonal sea ice zone south of the polar front. The photoperiods chosen were for the
203 months of August, November, January and March to represent winter sea ice, spring
204 meltwater, summer pelagic and autumn new ice conditions, respectively (Table 1).
205 Approximations of maximum daily irradiance values for the different months were derived
206 from the measurements of Lizotte and Sullivan (1991) that were taken at a similar (approx.
207 064°S) latitude (Table 1). Given missing data for January, summer maximum irradiance was
208 estimated to be 2000 μmol photons m^{-2} s^{-1} (Rozema et al 2001) assuming no cloud cover.
209 Irradiance within the water column or sea ice was estimated using Beer's Law:

210 $$I_Z = nI_O\, e^{-kz} \qquad (1)$$

where I_Z is the irradiance at depth z, I_O is incident irradiance, k is the light attenuation coefficient and *n* is the transmissivity of the interface between air and water or air and ice. The attenuation coefficients differed between environments (Table 1). For the meltwater and pelagic environments, k values were taken from Rasmus et al (2004) who measured attenuation from the marginal ice zone to the polar front in the range of 0.03 to 0.09 m^{-1}. The higher attenuation values were found at the ice edge and polar front due to increased phytoplankton biomass, with the lowest attenuation measured in intermediate pelagic waters (Rasmus et al 2004). Therefore, k values of 0.09 and 0.03 m^{-1} were used for the meltwater and pelagic environments, respectively (Table 1). For the sea ice environment a k value of 1.5 m^{-1} was used (Maykut 1985). To account for reflectance at the air-sea interface in the meltwater and pelagic environments, *n* was assumed equal to 0.95 (Gregg and Carder 1990, valid for solar zenith angles less than 45 degrees). To account for irradiance loss due to high albedo of snow and ice, *n* was set to 0.2 and 0.5 in the presence and absence of snow, respectively (Maykut 1985).

To better simulate fluctuating light conditions that result from strong vertical mixing, pelagic irradiance was determined at two depths (15 and 60 m) and values obtained from each were used interchangeably on a 1:1 h (high light: low light) cycle for the entire photoperiod (Fig. 2). It is recognised that the irradiance values are only model estimates for in situ irradiance that use over-simplified coefficients of extinction and albedo and that these modelled data fail to account for variations in absorption, reflection and scattering properties of snow, ice and water of differing composition.

Results

234 *Chlorophyll a fluorescence*

235 Relative electron transport rates ($rETR_{Chl}$) varied between all three species and all
236 environments (Fig. 3). There was more than a two-fold difference in $rETR_{Chl}$ for *F. cylindrus*
237 under the pelagic and sea ice conditions when compared with the other two species (Fig. 3).
238 *Pseudo-nitzschia subcurvata* showed minimal $rETR_{Chl}$ under sea ice-like conditions and
239 maximal rates under the low saline (meltwater) conditions (Fig. 3A, B). In contrast,
240 *Chaetoceros* sp. showed the reverse, with maximal $rETR_{Chl}$ in the sea ice and minimal rates
241 under pelagic conditions (Fig. 3A, C). Maximum rETR ($rETR_{max}$) was significantly different
242 between all three species across all three salinity and temperature treatments ($P < 0.001$). It
243 was consistently higher in *F. cylindrus* in all environments with highest values measured
244 under the conditions similar to sea ice (Table 2). For *P. subcurvata* values of $rETR_{max}$ were
245 lowest under the sea ice conditions and highest in meltwater conditions (Table 2). A
246 decreasing trend from sea ice to the pelagic environment was measured in *Chaetoceros* sp..
247 There were significant differences in light utilisation efficiency (α_{ETR}) between environmental
248 conditions ($P = 0.001$) and between all three species ($P < 0.001$), with the highest α_{ETR}
249 measured in both *F. cylindrus* and *Chaetoceros* sp. acclimated to sea ice conditions (Table 2),
250 while in *P. subcurvata* the highest value was measured under meltwater conditions (Table 2).
251 Minimum saturating irradiances (E_{KETR}) varied significantly between species ($P < 0.001$) and
252 across the three environments ($P = 0.001$). In all three environments, E_{KETR} was greatest in *F.*
253 *cylindrus* increasing from the sea ice to the pelagic environment. Minimum saturating
254 irradiance levels were relatively similar in the other two species. There was an increasing
255 trend from the sea ice to the pelagic environment for *P. subcurvata*, but no difference in
256 E_{KETR} for *Chaetoceros* sp. between the three environments (Fig. 3; Table 2).

257

258 *Oxygen evolution*

259 The oxygen data showed very similar patterns to the $rETR_{Chl}$ light response curves
260 with clear variations between all three species under all three environments (Fig. 4). Again,
261 there was more than a two-fold difference in net primary production for *F. cylindrus* under
262 the pelagic and sea ice conditions when compared with the other two species (Fig. 4). As with
263 the fluorescence data, *P. subcurvata* showed minimal net primary production under sea ice
264 conditions and maximal rates under meltwater conditions (Fig. 4A, B). In contrast,
265 *Chaetoceros* sp. showed a decreasing trend in oxygen evolution rates from the sea ice to the
266 pelagic environment (Fig. 4). Maximum oxygen evolution (O_{2max}) was significantly different
267 between all three species across all three treatments ($P < 0.001$) and was consistently higher
268 in *F. cylindrus* under all environmental conditions (Table 2). There were significant
269 differences in light utilisation efficiency (α_{O2}) between environmental conditions across the
270 three species ($P < 0.001$), with the highest α_{O2} measured in both *F. cylindrus* and
271 *Chaetoceros* sp. acclimated to sea ice conditions (Table 2). As with the fluorescence data, the
272 highest α_{O2} value was measured under meltwater conditions for *P. subcurvata* (Table 2).
273 Minimum saturating irradiances ($E_{K\,O2}$) varied significantly between species across the three
274 environments ($P < 0.001$). In all three environments, $E_{K\,O2}$ was greatest in *F. cylindrus* and
275 increased from the sea ice to the pelagic environments. In the other two species, $E_{K\,O2}$ was
276 lowest under sea ice conditions and maximal in the meltwater environment (Fig. 4; Table 2).

277

278 *Optimal irradiance and photoinhibition*

279 Optimal photosynthetic irradiance ($E_{M\,O2}$) in *F. cylindrus* was approximately double
280 the minimum saturating irradiance values under each environmental condition and like E_{KO2}

281 (Table 2), increased from the sea ice to the pelagic environmental conditions (Table 3). In *P.*
282 *subcurvata* there was no difference in $E_{M\,O2}$ between environmental conditions, whereas for
283 *Chaetoceros* sp., optimal irradiance was greatest under meltwater and lowest in the sea ice
284 conditions (Table 3). Photoinhibitory irradiance ($E_{B\,O2}$) revealed photoinhibition in all species
285 under all environmental conditions (Fig. 4; Table 3). The greatest photoinhibition was
286 measured in the meltwater and lowest under sea ice conditions for *F. cylindrus*. It increased
287 from the sea ice to the pelagic environment in *P. subcurvata* and was lowest under meltwater
288 conditions for *Chaetoceros* sp. (Table 3).

289

290 *Oxygen versus fluorescence based net primary production*

291 Oxygen evolution and rETR plotted together as a function of light showed good
292 correlation at irradiances below E_K, but considerable differences in shape of the curve at
293 higher irradiances (Fig. 5). The pooled oxygen and fluorescence data for all species under all
294 environmental conditions showed a significant correlation between the linear component of
295 the fluorescence and oxygen data ($R^2 = 0.8392$, $P = 0.0001$; Fig. 6, regression A). However,
296 the remaining data for irradiance levels well above E_K for each species was not significant
297 (Fig 6, regression B).

298

299 *Salinity and temperature responses*

300 The complete matrix of photosynthetic parameters determined from the oxygen data,
301 α_{O2}, O_{2max}, and $E_{K\,O2}$ in response to changes in salinity and temperature, revealed differences
302 between the three diatom species (Fig. 7). *Fragilariopsis cylindrus* and *Chaetoceros* sp.
303 showed high light utilisation efficiency (α_{O2}) in the low to mid-range temperatures and mid-

304 to high salinities (Fig. 7A, C), whereas *P. subcurvata* showed a preference for the
305 intermediate to high temperatures and lower salinities (Fig. 7B). Maximum photosynthesis
306 (O_{2max}) varied across the three species, with *F. cylindrus* yielding maximum values at mid- to
307 high salinities and warmer temperatures (Fig. 7D). *Fragilariopsis cylindrus* showed a salinity
308 threshold in which high rates of photosynthesis began to decline unless temperature also
309 decreased (Fig. 7D). In *P. subcurvata* photosynthetic activity (O_{2max}) was optimal at lower
310 salinities and warmer conditions (Fig. 7E), while for *Chaetoceros* sp., maximum
311 photosynthesis occurred at higher salinities and mid-range temperatures (Fig. 7F). Minimum
312 light saturation values ($E_{K\,O2}$) were highest in warmer temperatures for all three species;
313 however there were some differences in salinity sensitivity between species. *Fragilariopsis*
314 *cylindrus* showed high values across a range of salinities (Fig. 7G), whereas in *P. subcurvata*
315 the lowest salinities yielded the highest saturating irradiances (Fig. 7H). *Chaetoceros* sp.
316 showed higher minimum light saturation values at the higher salinities (Fig. 7I).

317

318 *Estimated daily net primary production: species, environment and light climate*

319 Daily estimates of integrated net primary production determined from the modelled
320 integrated PAR for each environment (Fig. 2) showed *F. cylindrus* with the highest
321 productivity of all three species under all environments (Fig. 8). *Fragilariopsis cylindrus*
322 showed a light-dependent response, with low values in the winter sea ice and very high
323 values in the meltwater, pelagic and newly formed ice environments (Fig. 8). Net primary
324 production was strongly inhibited in *P. subcurvata* under sea ice conditions at both high and
325 low irradiances, however rates of NPP were highest under the higher irradiances combined
326 with lower salinities and warmer temperatures of the meltwater and pelagic environments
327 (Fig. 8). Daily estimates of net primary production for *Chaetoceros* sp. were much lower in

328 the meltwater environment compared with the other two species, but followed the same light-
329 dependent pattern as *F. cylindrus* with the highest rates estimated for the pelagic environment
330 (Fig. 8).

331

332 Discussion

333 Microalgae exposed to variable environments generally possess the capacity for rapid
334 acclimation and a highly plastic photosynthetic apparatus (Kolber et al 1988). All three
335 species of Antarctic diatoms exhibited photophysiological plasticity by their ability to
336 acclimate to the rapid shift in environmental condition. Each diatom showed different
337 physiological responses that correlated well with their known distribution, displaying
338 physiological preferences for one particular niche environment over another. The
339 photosynthetic parameters obtained from the oxygen measurements showed similarity in the
340 patterns to those obtained from the fluorescence data (Table 2). However, there were some
341 differences between the fluorescence and oxygen measurements including maximum
342 photosynthesis in *F. cylindrus* (Table 2). According to oxygen measurements, O_{2max} occurred
343 under pelagic conditions, yet $rETR_{max,}$ based on fluorescence data, occurred under sea ice
344 conditions, which could be due to the presence of alternative electron cycling (AEC).

345 The variability in accessory pigments and physiological properties between species
346 means that there is considerable heterogeneity in light utilisation efficiency within a
347 phytoplankton community (Wilhelm et al 1990). The higher rates of light utilisation
348 efficiency (α) in *F. cylindrus* and *Chaetoceros* sp. under sea ice conditions, suggest an
349 increase in light capturing capacity by the antenna of PSII, which would explain light
350 saturation occurring at lower irradiances in these two species. In contrast, the small α under

sea ice conditions measured in *P. subcurvata* suggests a smaller PSII antenna, and explains the high irradiance required to reach photosynthetic saturation compared with the other environmental conditions (Juneau and Harrison 2005). The lower α values measured in *P. subcurvata* under all three environmental conditions is likely due to it being a much larger cell (approx. 50 μm vs 5 μm) and therefore having much higher chlorophyll *a* content, leading to increased packaging effect and lower photoprotective capacity (Dimier et al 2009). This suggests that this species would display maximum efficiency under stable light climates, such as those provided by the meltwater environment (Dierssen et al 2002), which was indeed observed in this study.

Values of $E_{K\,O2}$ ranged between 37 and 163 μmol photons m^{-2} s^{-1} which are consistent with Antarctic phytoplankton both from the pack ice (Lizotte and Sullivan 1991; Dower et al 1996) and pelagic environments (Tilzer et al 1986; Brightman and Smith 1989). Saturating irradiance is an indicator of photoadaptation, changing as a result of light history and thereby helping to identify shade- vs light-adapted species. The increase in E_K from the sea ice to the open ocean in *F. cylindrus* suggests that this species is well-adapted to sea ice conditions in which light levels are rarely as high in comparison to the meltwater or pelagic environments (Palmisano et al 1987). By maximising light utilisation efficiency and not light absorption capacity—since light levels are rarely excessive—*F. cylindrus* can optimise photosynthesis in the sea ice environment. Additionally, *F. cylindrus* is well-adapted to the other environments, whereby reducing light captured by the PSII antenna, the photosystem can tolerate higher irradiances such as the levels occurring in the meltwater and pelagic environments. Light saturation did not vary greatly between environments for *P. subcurvata,* but was greatest in the meltwater environment. A higher E_K at lower salinities is indicative of a reduced capacity for low light acclimation (Arrigo and Sullivan 1992), which makes sense for *P. subcurvata*

given the reduced light utilisation efficiency observed. Similarly, both oxygen and fluorescence data revealed *Chaetoceros* sp. to exhibit the highest light saturation under meltwater conditions and not pelagic conditions, as was found in *F. cylindrus*. The seemingly contradictory higher O_2 evolution (O_{2max}) under sea ice conditions may be the result of greater light respiration at the warmer temperatures. Previous work on another Antarctic *Chaetoceros* sp. showed that lower temperatures (-1.5°C) resulted in more efficient carbon assimilation and less respiratory losses (Thomas et al 1992). Although *Chaetoceros* sp. showed similar light utilisation efficiency (α) under sea ice conditions as *F. cylindrus*, E_K was much lower, suggesting greater sensitivity to sea ice conditions and different light harvesting capacity.

The trends in E_K were the same in the fluorescence and oxygen measurements, but there were large differences in the actual values, where E_K determined from rETR were much higher than those obtained from the oxygen measurements (Fig. 4; Table 2). Such differences have been measured, with PSII electron transport determined E_K exceeding values determined by oxygen evolution rates (Prasil et al 1996; Gilbert et al 2000; Wagner et al 2006). This is due to the fact that oxygen evolution measures net photosynthesis, whereas fluorescence-based rETR represents gross PSII-dependent electron transport, failing to differentiate between electrons derived from water-splitting with electrons being re-cycled through photosystem II (Genty et al 1989). While no direct measurement of cyclic electron transport of PSII were made in this study, it seems highly likely that the difference in the shape of the light response curves and E_K values based on fluorescence and oxygen measurements can be attributed to the non-oxygen consuming process of cyclic electron transport around PSII (Prasil et al 1996; Lavaud et al 2002). The advantage to cyclic electron transport is that it can be switched on faster than heat dissipation via non-photochemical quenching (Onno Feikema

et al 2006) and allows the cell to maintain maximum photosynthetic capacity while keeping energy-dependent quenching minimal (Lavaud 2007).

Relative ETR and α are temperature-dependent processes (Palmisano et al 1987; Arrigo and Sullivan 1992) however, only *Chaetoceros* sp. expressed such a response in this study (Table 2). Instead, a salinity trend was detected. Using the ^{14}C method, Arrigo and Sullivan (1992) found rETR and α parameters to increase with increasing salinity up to 50 before declining again in Antarctic sea ice algal populations. A similar salinity trend was detected in this study, where rETR and α were highest in the sea ice and lowest in the meltwater environments for *F. cylindrus* (Table 2). This same trend was observed in α, determined from the oxygen data, in *Chaetoceros* sp. (Table 2). However, for *P. subcurvata*, maximum values of all parameters were detected under meltwater conditions, further implying adaptation to lower salinities. This response correlates well with a previous study where increased salinity retarded growth more than lowered temperatures (Aletsee and Jahnke 1992) assuming photosynthetic activity as a proxy for growth.

Phytoplankton photosynthetic efficiency is influenced by both temperature and salinity, as both factors affect rates of photosynthesis. Factors can act independently (one has an effect, while the other doesn't), synergistically (the combined affect is greater than the individual) or antagonistically (where one stress offsets the damage of the other). Interactive effects between temperature and salinity were detected in *F. cylindrus*, where elevated salinity mitigated the effects of lower temperatures (Fig. 7). This demonstrates a situation in which multiple stressors, rather than causing a synergistic effect, can actually be less stressful than the individual stress. These data suggest that this mitigative response in *F. cylindrus* is linked with a greater adaptability to the sea ice environment (which naturally has simultaneously low temperatures and high salinities), supporting the observed dominance of

this species in the Antarctic sea ice. In contrast, the same combination of low temperature and high salinity in *P. subcurvata* yielded low, α_{O2}, O_{2max}, and $E_{K\,O2}$ values having more of a negative effect. At low salinities and warmer temperatures, *P. subcurvata* showed less photosynthetic stress, indicating temperature and salinity sensitivity and suggesting that its preferred ecological niche is somewhere between meltwater and pelagic conditions (Fig. 7). *Chaetoceros* sp. responded in a similar manner as *F. cylindrus*, but showed greater sensitivity towards low salinities, a situation in which an individual factor is responsible for negative responses alone.

It should be noted that this study compared acclimation capacity after only 3 days, and therefore cannot rule out the possibility that all species could in fact acclimate successfully to all conditions given more time. However, what this study does highlight is that there are species-specific differences in rapid acclimation capacity, which could have implications for an ecological competitive advantage. In addition, it must be noted that the short-term (72 h) acclimation period used in this study may have led to the experimental conditions slightly over-estimated the stress of the sea ice environment, as the shift from growth environment (+4˚C at 34) to the low temperature/high salinity sea ice conditions (-1.5˚C at 70) would likely take longer to reach acclimation than to the meltwater conditions (+2˚C at 32). However, this would not have affected differences in the short-term acclimation capacity between the three species.

Daily integrated NPP was greatest in the summer pelagic environment and lowest under the winter sea ice conditions for *F. cylindrus* and *Chaetoceros* sp., while maximal NPP was calculated for *P. subcurvata* under meltwater conditions (Fig. 8). The light-dependent response of *F. cylindrus* and *Chaetoceros* sp. highlights the strong link between light availability and NPP. For these two species, low irradiances limited the amount of active

photosynthesis. In contrast, *P. subcurvata* showed an interactive effect of salinity and temperature with light, where the low temperature and high salinities of the sea ice environments drastically reduced NPP regardless of available irradiance. It is important to note that the growth irradiance in this experiment was not representative of field conditions and was instead kept constant throughout the salinity and temperature manipulations, potentially influencing the photoacclimation potential of the phytoplankton. Furthermore, the irradiance level used was below light saturation for photosynthesis in all species under all environmental conditions. Thus, it is possible that when acclimated to different light intensities, the diatoms may show entirely different photosynthesis versus irradiance characteristics, particularly with respect to photochemical efficiency at low irradiances and photoinhibition at higher light levels. Future studies should aim to combine light, temperature and salinity shifts to provide greater insight into the true photoacclimation potential and NPP of each species.Photoinhibition was not great enough to affect the light-dependent response of NPP in this study, but this could be an artefact of the constant photon fluence rates used. The greatest average daily irradiance of 232 μmol photons m^{-2} s^{-1} in the pelagic environment resulted in the highest NPP regardless of high photoinhibition, with the exception of *P. subcurvata*, where salinity concentrations and constant high light had a greater influence over NPP (Fig. 8). Even with the fluctuations in light, the total irradiance was still greater than in the meltwater environment. Photoinhibition was present under all conditions with the exception of the winter sea ice scenario, which had a calculated daily mean irradiance of just 3.4 μmol photons m^{-2} s^{-1}. Therefore, the contribution of photoinhibition can be entirely ignored in the winter sea ice scenario. However, the low NPP values for *P. subcurvata* in both (autumn/early spring) sea ice environments is indicative of sensitivity to the high salinity and low temperatures, but also shows high light adaptation and limited photosynthetic plasticity for low light conditions. The higher NPP values of *P. subcurvata*

compared to *Chaetoceros* sp. in the high light meltwater conditions is largely due to higher photoinhibition in *Chaetoceros* sp.. Whereas values are relatively similar in the pelagic waters as a result of the intermittent low light that drastically lowers NPP in *P. subcurvata*.

While there are many recognised limitations to these modelled data, the derived values of NPP are consistent with the fluorescence and oxygen physiological data and all tell a similar story. *Fragilariopsis cylindrus* possesses a highly plastic photosystem and while well-adapted for the sea ice environment, remains the most productive species under all three conditions. Based on this study, the results show that *F. cylindrus* is able to acclimate to the new salinity and temperature conditions more rapidly than the other two species, potentially giving it a competitive advantage in the marine environment. This strongly supports its wide distribution as a generalist species and upholds its prevalence throughout the Antarctic marine ecosystem (Lizotte, 2001; Kopczynska et al., 2007; Roberts et al., 2007; Beans et al., 2008). In contrast, *P. subcurvata* showed a particular adaptation to meltwater characteristics with a much lower level of photosynthetic plasticity for changes in salinity, temperature and light, perfectly matching its geographical environment of known greatest abundance (Almandoz et al., 2008). Finally, *Chaetoceros* sp. expressed an ability to adjust to sea ice conditions, but displayed a clear preference toward the more pelagic environment with sensitivity to low saline conditions, correlating with its known distribution in the Antarctic coastal pelagic environment.

Knowledge of species-specific photosynthetic capacity is essential to obtain good estimates of primary productivity (Juneau and Harrison 2005). This study has shown that photosynthesis in three Antarctic diatoms is sensitive to rapid changes in temperature and salinity that occur in the Antarctic ecosystem during an annual cycle. Better understanding the influence these changes can have on photosynthesis and NPP may shed some light on the

physiological mechanism controlling the distribution of phytoplankton in the Antarctic marine environment. The species-specific sensitivities to changes in salinity and temperature uncovered in this study have strengthened the link between phytoplankton photosynthetic capacity and ecological niche occupancy.

515 Acknowledgements

516 Thanks to the three anonymous reviewers for their input to improve this paper.
517 Thanks to Olivia Sackett for experimental assistance and Dr Isabel Jimenez-Denness for her
518 support, helpful discussions and guidance. We are grateful to Dr A. Pankowski, Dr P. Assmy
519 and Dr C. Hassler for supplying the three Antarctic cultures (*F. cylindrus, P. subcurvata* and
520 *Chaetoceros* sp., respectively). Financial support was provided by the Australian Research
521 Council grant (DP0773558) awarded to PJR, Aquatic Processes Group and Department of
522 Environmental Sciences, University of Technology, Sydney. KP was supported by an
523 Australian Postgraduate Award and the Commonwealth Scientific and Industrial Research
524 Organisation (CSIRO) top-up scholarship.

525

526

527

528

529

530

531

532

533

534

535

536 References

537 Aletsee L, Jahnke J (1992) Growth and productivity of the psycro- philic marine diatoms
538 *Thalassiosira antarctica* Comber and *Nitzschiafriqida* Grunow in batch cultures at
539 temperatures below the freezing point of sea water. Pol Biol 11:643-647

540 Almandoz GO, Ferreyra GA, Schloss IR, Dogliotti AI, Rupolo V, Paparazzo FE, Esteves JL,
541 Ferrario ME (2008) Distribution and ecology of *Pseudo-nitzschia* species
542 (Bacillariophyceae) in surface waters of the Weddell Sea (Antarctica). Pol Biol 31:429-
543 442

544 Arrigo K, Sullivan CW (1992) The influence of salinity and temperature covarioation on the
545 photophysiological characteristics of Antarctic sea ice microalgae. J Phycol 28:746-756

546 Bailey S, Melis A, Mackey KRM, Cardol P, G F, van Dijken G, Berg G, Arrigo KR, Shrager
547 J, Grossman A (2008) Alternative photosynthetic electron flow to oxygen in marine
548 *Synechococcus*. Biochim Biophys Acta 1777:269-276

549 Beans C, Hecq JH, Koubbi P, Vallet C, Wright S, Goffart A (2008) A study of the diatom-
550 dominated microplankton summer assemblages in coastal waters from Terre Ade´lie to
551 the Mertz Glacier, East Antarctica (139E–145E). Pol Biol 31:1101-1117

552 Bendall D, Manasse R (1995) Cyclic photophosphorylation and electron transport. Biochim
553 Biophys Acta 1229:23-38

554 Brightman R, Smith WO (1989) Photosynthesis-irradiance relationships of Antarctic
555 phytoplankton during austral winter. Mar Ecol Prog Ser 53:143-151

556 Dierssen HM, Smith RC, Vernet M (2002) Glacial meltwater dynamics in coastal waters west
557 of the Antarctic peninsula. PNAS 99:1790-1795

558 Dimier C, Corato F, Tramontano F, Brunet C (2007) Photoprotection and xanthophyll-cycle
559 activity in three marine diatoms. J Phycol 43:937-947

560 Dimier C, Giovanni S, Ferdinando T, Brunet C (2009) Comparative Ecophysiology of the
561 Xanthophyll Cycle in Six Marine Phytoplanktonic Species. Protist 160:397-411
562 Dower KM, Lucas MI, Phillips R, Dieckmann G, Robinson DH (1996) Phytoplankton
563 biomass, P-I relationships and primary production in the Weddell Sea, Antarctica,
564 during the austral autumn. Pol Biol 16:41-52
565 Eicken H (1992) The role of sea ice in structuring Antarctic ecosystems. Pol Biol 12:3-13
566 Geel C, Versluis W, Snel JFH (1997) Estimation of oxygen evolution by marine
567 phytoplankton from measurement of the efficiency of Photosystem II electron flow.
568 Photosynth Res 51:61-70
569 Genty B, Briantais J-M, Baker NR (1989) The relationship between the quantum yield of
570 photosynthetic electron transport and quenching of chlorophyll fluorescence. Biochim
571 Biophys Acta 990:87-92
572 Gilbert M, Domin A, Becker A, Wilhelm C (2000) Estimation of Primary Productivity by
573 Chlorophyll a in vivo Fluorescence in Freshwater Phytoplankton. Photosynthetica
574 38:111-126
575 Gleitz M, Thomas DN (1992) Physiological responses of a small Antarctic diatom
576 (Chaetoceros sp.) to simulated environmental constraints associated with sea-ice
577 formation. Mar Ecol Prog Ser 88:271-278
578 Gregg W, Carder KL (1990) A simple spectral solar irradiance model for cloudless maritime
579 atmospheres. Limnol Oceanogr 35:1657-1675
580 Guillard RR, Ryther JH (1962) Studies of marine planktonic diatoms I. *Cyclotella nana*
581 Hudstedt and *Detonula confervacea* Cleve. Can J Microbiol 8:229-239
582 Juneau P, Harrison P (2005) Comparison by PAM Fluorometry of photosynthetic activity of
583 nine marine phytoplankton grown under identical conditions. Photochem Photobiol
584 81:649-653

585 Kashino Y, Kudoh S, Hayashi Y, Suzuki Y, Odate T, Hirawake T, Satoh K, Fukuchi M
586 (2002) Strategies of phytoplankton to perform effective photosynthesis in the North
587 Water. Deep-Sea Res II 49:5049-5061
588 Kolber ZS, Prasil O, Falkowski PG (1998) Measurements of variable chlorophyll
589 fluorescence using fast repetition rate techniques: defining methodology and
590 experimental protocols. Biochimica et Biophysica Acta (BBA) - Bioenergetics
591 1367:88-106
592 Kopczynska EE, Savoye N, Dehairs F, Cardinal D, Elskens M (2007) Spring phytoplankton
593 assemblages in the Southern Ocean between Australia and Antarctica. Pol Biol 31:77-
594 88
595 Krause GH, Weis E (1991) Chlorophyll Fluorescence and Photosynthesis: The Basics. Ann
596 Rev Plant Physiol Plant Mol Biol 42:313-349
597 Lavaud J, Strzepek R, Kroth PG (2007) Photoprotection capacity differs among diatoms:
598 Possible consequences on the spatial distribution of diatoms related to fluctuations in
599 the underwater light climate. Limnol Oceanogr 52:1188-1194
600 Lavaud J, van Gorkom H, Etienne A-L (2002) Photosystem II electron transfer cycle and
601 chlororespiration in planktonic diatoms. Photosynth Res 74:51-59
602 Lizotte MP (2001) The Contributions of Sea Ice Algae to Antarctic Marine Primary
603 Production. Amer Zool 41:57-73
604 Lizotte MP, Sullivan CW (1991) Photosynthesis-irradiance relationships in microalgae
605 associated with Antarctic pack ice: evidence for in situ activity. Mar Ecol Prog Ser
606 71:175-184
607 Mackey K, Paytan A, Grossman A, Bailey S (2008) A photosynthetic strategy for coping in a
608 high-light, low nutrient environment. Limnol Oceanogr 53:900-913

609 Masojidek J, Grobbelaar J, Pechar L, Koblizek M (2001) Photosystem II electron transport
610 rates and oxygen production in natural waterblooms of freshwater cyanobacteria during
611 a diel cycle. J Plankton Res 23:57-66
612 Maykut GA (1985) The Ice Environment. In: Horner RA (ed) Sea Ice Biota. CRC Press,
613 Boca Raton, p 21-82
614 Onno Feikema W, Marosvölgyi MA, Lavaud J, van Gorkom HJ (2006) Cyclic electron
615 transfer in photosystem II in the marine diatom *Phaeodactylum tricornutum*. Biochim
616 Biophys Acta 1757:829-834
617 Palmisano AC, SooHoo JB, Sullivan CW (1987) Effects of four environmental variables on
618 photosynthesis-irradiance relationships in Antarctic sea-ice microalgae. Mar Biol
619 94:299-306
620 Prasil O, Kolber Z, Berry JA, Falkowski PG (1996) Cyclic electron flow around Photosystem
621 II in vivo. Photosynth Res 48:395-410
622 Ralph PJ, Gademann R (2005) Rapid light curves: A powerful tool to assess photosynthetic
623 activity. Aquat Bot 82:222-237
624 Rasmus KE, Graneli W, Wangberg SA (2004) Optical studies in the Southern Ocean. Deep
625 Sea Res Part II 51:2583-2597
626 Ritchie R (2006) Consistent Sets of Spectrophotometric Chlorophyll Equations for Acetone,
627 Methanol and Ethanol Solvents. Photosynth Res 89:27-41
628 Roberts D, Craven M, Cai M, Allison I, Nash G (2007) Protists in the marine ice of the
629 Amery Ice Shelf, East Antarctica. Pol Biol 30:143-153
630 Rozema J, Broekman R, Lud D, Huiskes A, Moerdijk T, de Bakker N, Meijkamp B, van
631 Beem A (2001) Consequences of depletion of stratospheric ozone for terrestrial
632 Antarctic ecosystems: the response of *Deschampsia antarctica* to enhanced UV-B
633 radiation in a controlled environment. Plant Ecol 154:103-115

Sakshaug E, Demers S, Yentsch CM (1987) *Thalassiosira oceanica* and *T. pseudonana*: two different photoadaptational responses. Mar Ecol Prog Ser 41:275-282

Strzepek RF, Harrison PJ (2004) Photosynthetic architecture differs in coastal and oceanic diatoms. Nature 431:689-692

Thomas D, Baumann M, Gleitz M (1992) Efficiency of carbon assimilation and photoacclimation in a small unicellular Chaetoceros species from the Weddell Sea (Antarctica): Influence of temperature and irradiance. J Exp Mar Biol Ecol 157: 195-209

Thomas D, Gleitz M (1993) Allocation of photoassimilated carbon into major algal metabolite functions: variation in two diatom species isolated from the Weddell Sea (Antarctica). Pol Biol 13:281-286

Tilzer MM, Elbrachter M, Gieskes WW, Beese Br (1986) Light-temperature interactions in the control of photosynthesis in Antarctic phytoplankton. Pol Biol 5:105-111

Wagner HJ, T.; Wilhelm, C. (2006) Balancing the energy flow from captured light to biomass under fluctuating light conditions. New Phytol 169:95-108

Wilhelm C (1990) The biochemistry and physiology of light-harvesting processes in chlorophyll b- and chlorophyll c-containing algae. Plant Physiol Biochem 28:293-306

Table 1. Summary of data used to model seasonal daily solar irradiance in the winter sea ice, meltwater, pelagic and new sea ice environments for estimations of NPP [μmol O_2 (mg chl *a*)$^{-1}$ d^{-1}] for *Fragilariopsis cylindrus*, *Pseudo-nitzschia subcurvata* and *Chaetoceros* sp..

Environment	Month	Photoperiod (h)[a]	Maximum I_O [b]	k (m^{-1})
Sea ice	August	8	150	1.5[d]
Meltwater	November	18.5	1500	0.09[e]
Pelagic	January	20	2000[c]	0.03[e]
New sea ice	March	13	1800	1.5[d]

[a] Obtained from www.esrl.noaa.gov/gmd/grad/solcalc for latitude 065°S and longitude 145°E

[b] Values are in µmol photons m^{-2} s^{-1} and were derived from Lizotte and Sullivan (1991)

[c] Estimated values assuming no cloud cover

[d] Light attenuation coefficient (k) for sea ice was taken from Maykut (1985)

[d] Light attenuation coefficients (k) obtained from Rasmus et al (2004)

673 Table 2. Photosynthetic parameters maximum electron transport rate (ETR_{max}), maximum oxygen evolution (O_{2max}), light utilisation
674 efficiency (α) and minimum saturating irradiance (E_K) calculated from light response curves of relative electron transport or oxygen
675 evolution according to Ralph and Gademann (2005). Data represent means for *Fragilariopsis cylindrus, Pseudo-nitzschia subcurvata*
676 and *Chaetoceros* sp.. ± SD (*n*=4).

		Light response curve of fluorescence			Light response curve of oxygen evolution		
Ecosystem	Species	$rETR_{max}$ [μmol e^- (mg chl *a*)$^{-1}$ h^{-1}]	α_{ETR}	E_{KETR} [μmol photons m^{-2} s^{-1}]	O_{2max} [μmol O_2 (mg chl *a*)$^{-1}$ h^{-1}]	α_{O2}	$E_{K\,O2}$ [μmol photons m^{-2} s^{-1}]
Sea ice	*F. cylindrus*	3105 ± 403	10.4 ± 3.7	315 ± 81	780 ± 105	12.8 ± 3.9	61 ± 3.6
	P. subcurvata	603 ± 76	4.6 ± 0.3	132 ± 24	332 ± 39.9	5.1 ± 0.7	44 ± 6.8
	Chaetoceros sp.	1577 ± 241	10.9 ± 1.6	144 ± 17	373 ± 61.9	10.0 ± 2.5	37 ± 2.3
Meltwater	*F. cylindrus*	1929 ± 526	4.73 ± 0.85	406 ± 66	470 ± 62	5.22 ± 1.3	89 ± 8.3
	P. subcurvata	1163 ± 149	6.38 ± 0.55	183 ± 28	449 ± 133	7.8 ± 1.4	57 ± 6.5
	Chaetoceros sp.	1265 ± 232	7.07 ± 0.31	178 ± 25	276 ± 90	4.1 ± 1.8	68 ± 11
Pelagic	*F. cylindrus*	2382 ± 307	5.70 ± 1.20	420 ± 106	1087 ± 106	6.07 ± 0.43	163 ± 3.6
	P. subcurvata	877 ± 79	3.95 ± 0.62	225 ± 35	346 ± 33	4.8 ± 1.7	50 ± 4
	Chaetoceros sp.	643 ± 55	4.44 ± 0.53	145 ± 73	270 ± 36	8.01 ± 0.93	56 ± 15

677

Table 3. Photosynthetic parameters optimal photosynthetic irradiance (E_M) and photoinhibitory irradiance (E_B) calculated from light response curves of oxygen evolution according to Ralph and Gademann (2005). Data represent means or *Fragilariopsis cylindrus*, *Pseudo-nitzschia subcurvata* and *Chaetoceros* sp. ± SD (*n*=4).

		Light response curve of oxygen evolution	
		$E_{M\ O2}$	$E_{B\ O2}$
Environment	Species	[μmol photons m^{-2} s^{-1}]	[μmol photons m^{-2} s^{-1}]
Sea ice	*F. cylindrus*	124 ± 10	138 ± 21
	P. subcurvata	62 ± 17	155 ± 35
	Chaetoceros sp.	36 ± 4.4	403 ± 192
Meltwater	*F. cylindrus*	185 ± 21	969 ± 77
	P. subcurvata	64 ± 38	554 ± 156
	Chaetoceros sp.	132 ± 31	201 ± 28
Pelagic	*F. cylindrus*	366 ± 9.8	367 ± 9.9
	P. subcurvata	48 ± 11	1077 ± 477
	Chaetoceros sp.	86 ± 38	756 ± 86

688 Figure legends

689 Figure 1. Spatial and temporal evolution and decay of sea ice in the Antarctic marine
690 ecosystem. Mixed layer depth and light attenuation are depicted. The seasonal pathway of
691 phytoplankton from the winter sea ice to the meltwater and pelagic environments are shown.
692 Temperature, salinity and irradiance properties for each environment are described in the
693 table below. Figure adapted from Eicken (1992).

694

695 Figure 2. Modelled daily in situ solar irradiance for microalgae in the sea ice (August - late
696 winter), meltwater (November - spring), pelagic (January - summer) and new sea ice (March
697 - autumn) environments at 065°S and 145°E. Fluctuations in irradiance are shown by the 1:1
698 h mixing pattern for PAR at 15 and 60 m.

699

700 Figure 3. Relative electron transport rates (rETR) as a function of irradiance in the Antarctic
701 diatoms *Fragilariopsis cylindrus*, *Pseudo-nitzschia subcurvata* and *Chaetoceros* sp. . under
702 A) sea ice B) meltwater and C) pelagic conditions. Maximum electron transport rate
703 (ETR_{max}), and saturating irradiance (E_{KETR}) are shown (dotted lines). Data represent mean ±
704 SD (n = 4).

705

706 Figure 4. Net primary production (measured as oxygen evolution) as a function of irradiance
707 in the Antarctic diatoms *Fragilariopsis cylindrus, Pseudo-nitzschia subcurvata* and
708 *Chaetoceros* sp. exposed to A) sea ice B) meltwater and C) pelagic conditions. Maximum

709 oxygen evolution rates (O_{2max}), and saturating irradiance (E_{KO2}) are shown (dotted lines).
710 Data represent mean ± SD (n = 4).

711

712 Figure 5. Comparison of light response curves for oxygen and fluorescence-based
713 photosynthesis in *Fragilariopsis cylindrus* under sea ice-like conditions. Light curves were
714 fitted according to Ralph and Gademann (2005). The relationship between rETR and O_2
715 evolution at low irradiance (initial points of light curve) are fitted with a linear regression
716 (inset). Data represent means ± SD (n = 4).

717

718 Figure 6. Correlation between pooled means of oxygen and fluorescence-based
719 photosynthesis of A) the values in the light curve below E_K (black circles) and B) remaining
720 points above E_K (white circles) after which the oxygen and fluorescence deviate. Data are
721 fitted with a linear regression. Data represent the mean of all species under sea ice meltwater
722 and pelagic conditions (n = 4).

723

724 Figure 7. Contour plots of the oxygen derived parameters α, O_{2max} [μmol O_2 (mg chl a)$^{-1}$ h^{-1}]
725 and E_K [μmol photons m^{-2} s^{-1}] in *Fragilariopsis cylindrus* (A, D, G), *Pseudo-nitzschia*
726 *subcurvata* (B, E, H) and *Chaetoceros* sp. (C, F, I) exposed to 31, 34, 55, and 70 at -1.5, +2
727 and +5°C.

728

729 Figure 8. Daily integrated net primary production as a function of modelled seasonal light
730 climate (see Fig. 2) in the sea ice (late winter), meltwater (spring), pelagic (summer) and new

731 sea ice (autumn) environments for Antarctic diatoms *Fragilariopsis cylindrus*, *Pseudo-*

732 *nitzschia. subcurvata* and *Chaetoceros* sp. exposed to altered salinity and temperature.

733

734

735

736

737

738

739

740

741

742

743

744

745

746

747

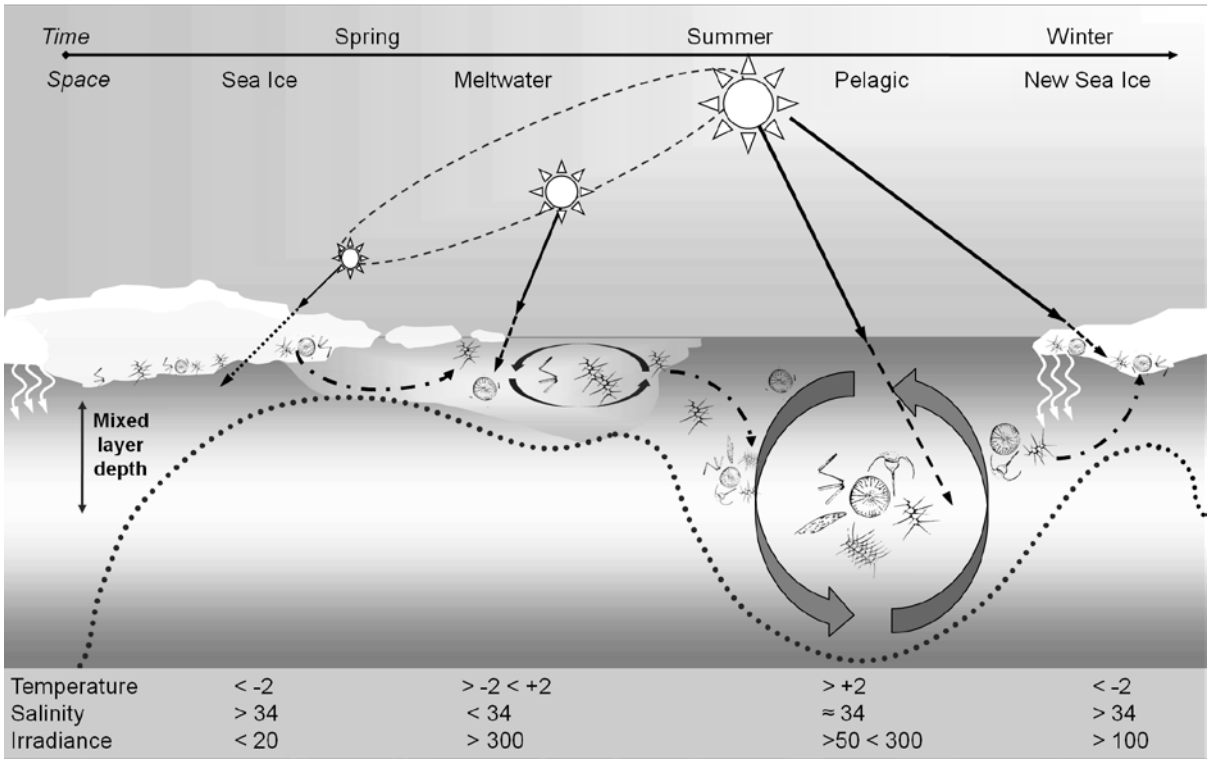

748

749

750

751

752

753

754

755

756

757

758 Fig. 1

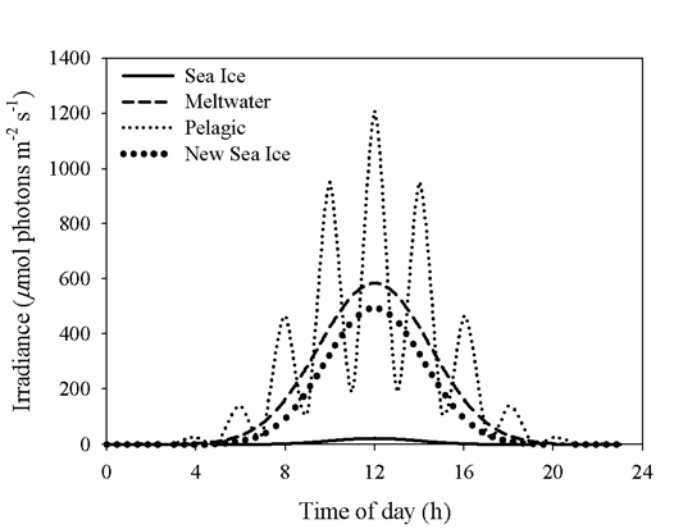

759

760

761

762

763

764

765

766

767

768

769

770

771 Fig. 2

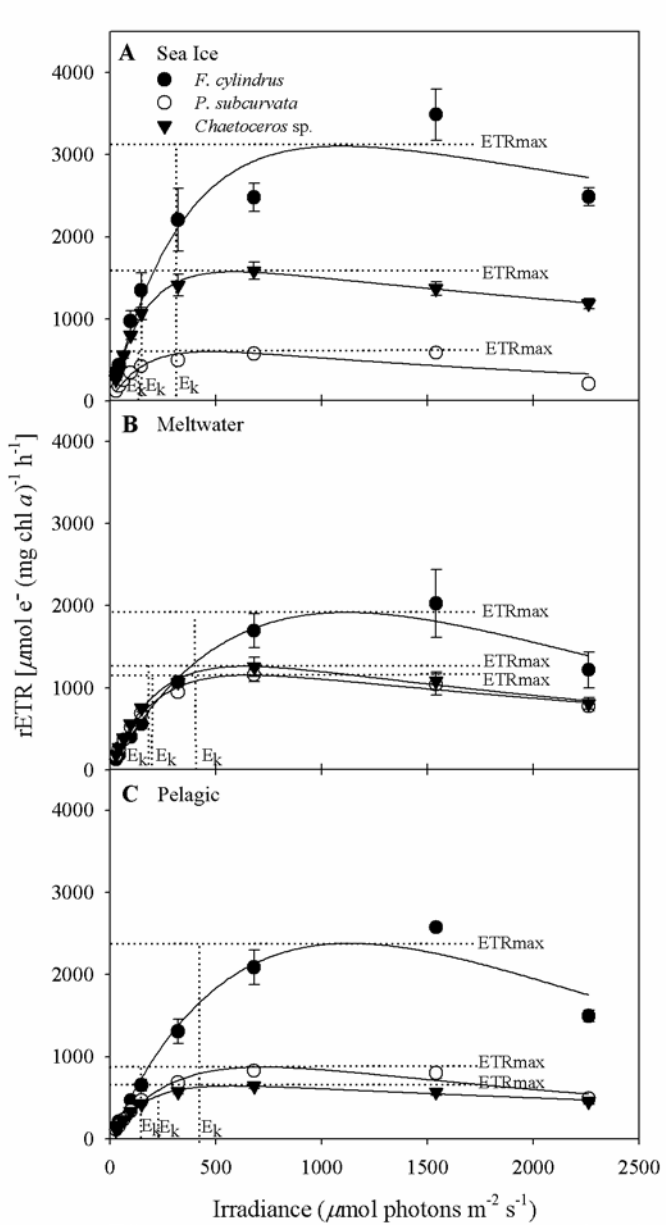

772

773

774

775

776

777 Fig. 3

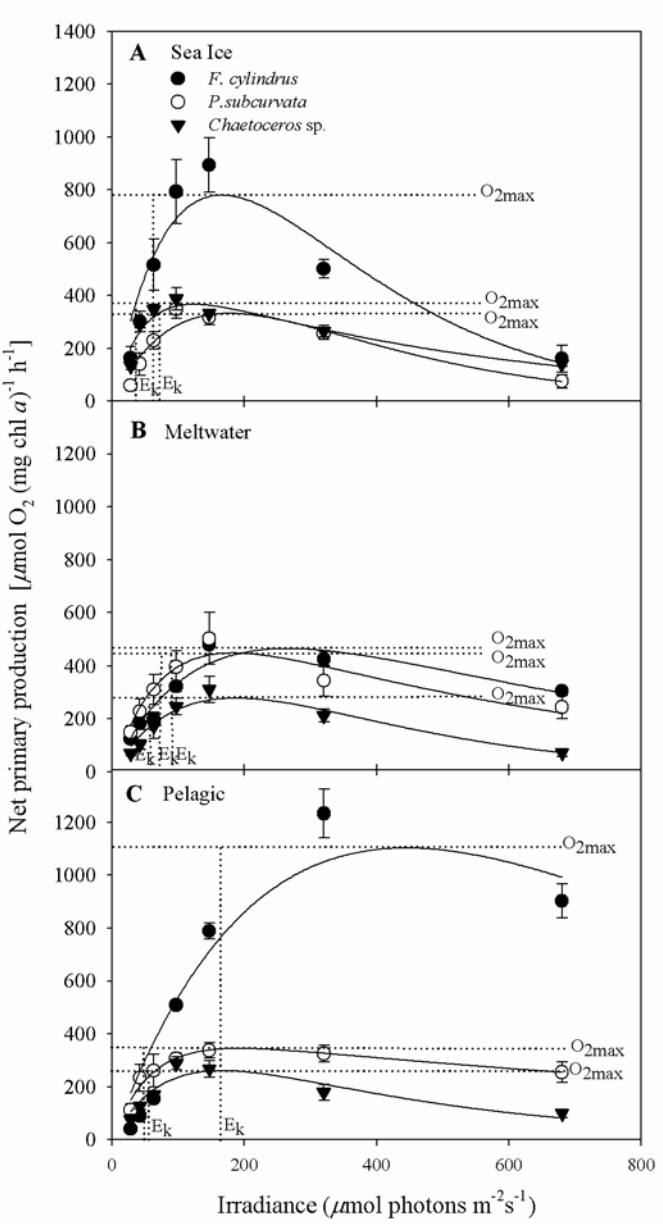

778

779

780

781

782

783

784 Fig. 4

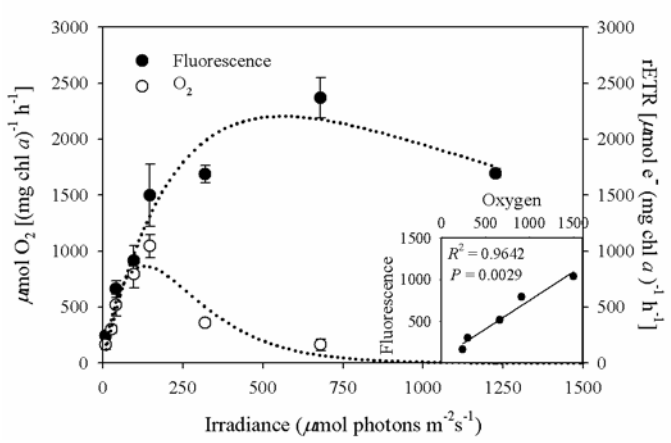
Fluorescence
O2
Oxygen
R2 = 0.9642
P = 0.0029
Fluorescence
µmol O2 [(mg chl a)-1 h-1]
rETR [µmol e- (mg chl a)-1 h-1]
Irradiance (µmol photons m-2s-1)

Fig. 5

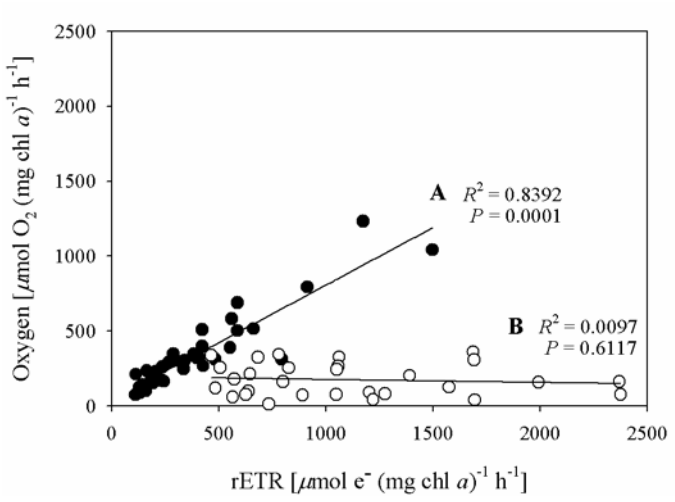

799

800

801

802

803

804

805

806

807

808

809

810

811 Fig. 6

812

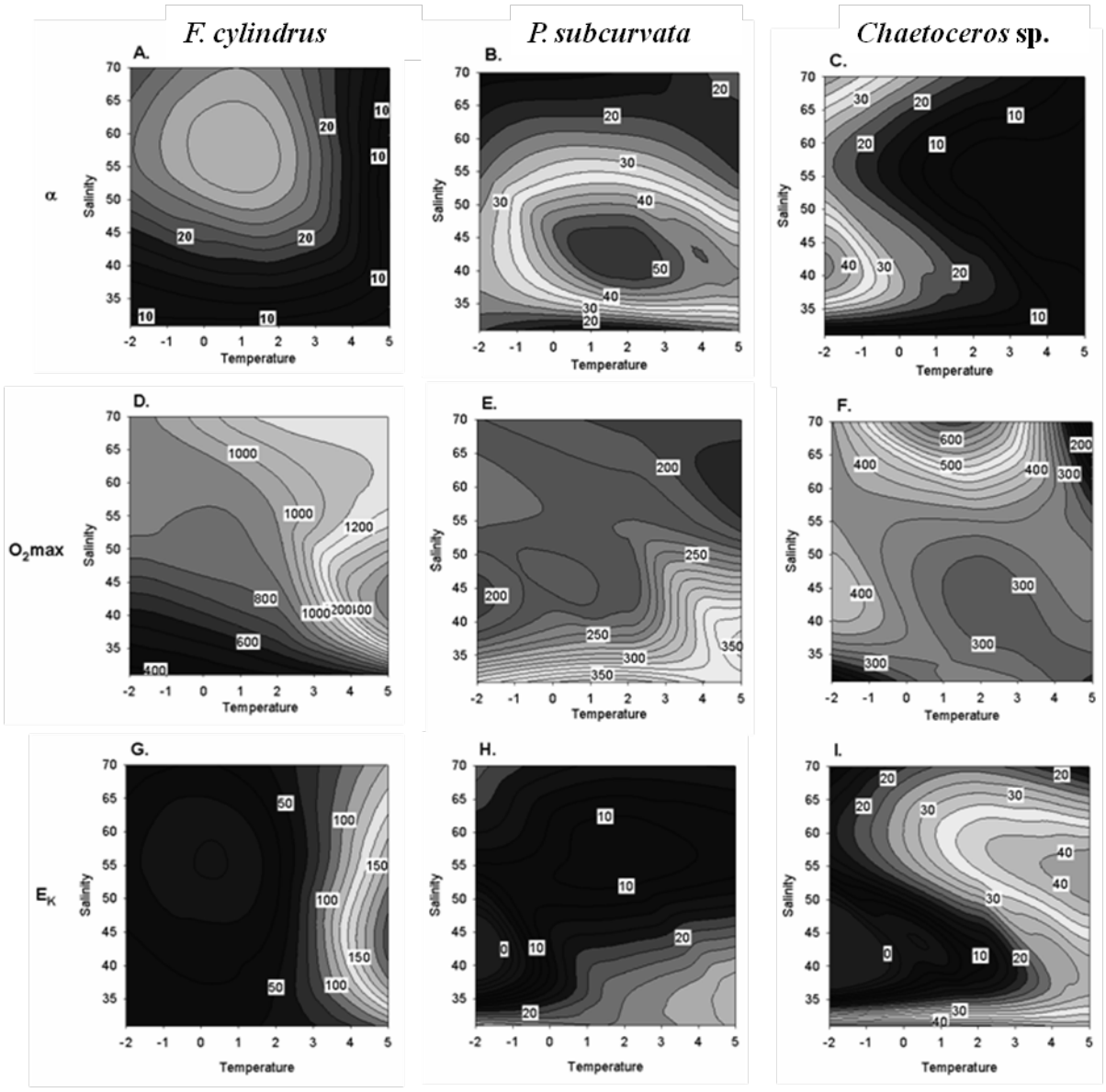

813

814

815

816

817

818

819 Fig. 7

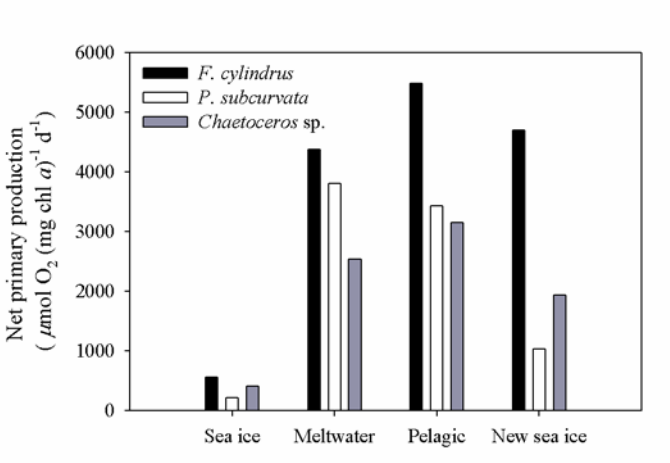

820

821

822

823

824

825

826

827

828

829

830

831

832

833 Fig. 8